Journal of Southeast University (English Edition) Vol. 40, No. 1, pp. 89 - 96 Mar. 2024 ISSN 1003—7985

Magnetic field and coupling effect analysis of a novel dual-rotor dual-stator permanent magnet synchronous generator

Fu Mingzhi[1] Qin Meng[1] Guo Xiaojiang[1] Chen Yuhan[2] Lin Heyun[2]

([1]Huaneng Clean Energy Research Institute, Beijing 100032, China)

([2]School of Electrical Engineering, Southeast University, Nanjing 210096, China)

Abstract: To tackle the issue of high cost and large volume for offshore wind power generators, a novel dual-rotor dual-stator permanent magnet synchronous generator (DRDS-PMSG) is proposed. The equivalent magnetic circuit model of the generator is established, finite element analysis is performed to evaluate the electromagnetic characteristics and coupling effect, and some simulation results are verified through experiment. The simulation analysis results show that three typical equivalent magnetic circuits exist with changed relative positions between the inner and outer magnets, and the equivalent reluctance of the coupling region can be described using a coupling coefficient. The coupling effect of inner and outer machines is revealed by electromagnetic characteristics, including cogging torque and electromagnetic torque. The peak-to-peak values of the cogging torque of inner and outer machines are 0.52 and 1.64 kN · m, the average values of electromagnetic torque are 11.65 and 27.09 kN · m, and the torque ripples are 6.02% and 4.12%, respectively. In general, a coupling effect exists between the inner and outer machines; however, the coupling effect is effectively reduced by the flux barrier.

Key words: dual-rotor dual-stator (DRDS); electromagnetic characteristics; permanent magnet synchronous generator (PMSG); magnetic field; finite element analysis; coupling effect

DOI: 10.3969/j.issn.1003 - 7985.2024.01.010

With the advancement of high-performance permanent magnet (PM) materials, the research and application of PM machines have experienced rapid development[1]. Meanwhile, the improvement in manufacturing technology and intelligent control strategy has laid a solid foundation for the study of dual-stator PM machines (DSPMMs) and dual-rotor PM machines (DRPMMs). These PM machines with relatively complex structures evolve from common PM machines and usually possess an extra stator or rotor to fully utilize the internal spaces. Consequently, the torque and power densities of such machines experience great enhancement, thus raising the machine's capacity without increasing its size and weight. Therefore, the design of PM synchronous generators (PMSGs) with a larger capacity becomes feasible, and energy saving and high efficiency show enormous potential in the field of wind power generation[2-3].

In recent years, many global scholars have proposed various novel topologies of DSPMMs and DRPMMs and have conducted prototype tests to improve their performance, thus providing theoretical and experimental reference to the real application of the machines in different operating conditions. A dual-stator five-phase PMSG was proposed for wind power generation, wherein a pseudo-pole was used to save PM materials. The magnetic circuit model of the machine was obtained, and the electromagnetic performance of the machine was analyzed and compared with that of dual-stator embedded-pole and single-stator single-rotor PMSG[4]. Kim et al.[5] designed a dual-stator radial-flux PM generator applied in wind turbines along with stator teeth pairing for the cancellation of its cogging torque. Another dual-stator PM generator was proposed for the applications in low-speed conditions, and the cogging torque was reduced through stator teeth pairing and pole-arc ratio adjustment[6]. Concurrently, DSPMMs with other structures are also investigated. A dual-stator axial-flux PM machine with soft magnetic composite cores was explored and optimized to meet the requirements for torque density in a robot servo system[7]. Certain machines with rare structures are also classified as DSPMMs, including the dual-stator flux-switching PM motor proposed in Ref. [8], where the PMs and windings are located on the stator, and a double-salient rotor is used to reduce the difficulty in manufacturing. Different rotor configurations of DSPMMs using superconducting (SC) material have also been explored to improve power capacity and reduce cogging torque and losses of large generators[9]. Allahyari et al.[10] proposed a consequent-pole DRPM vernier machine, wherein the windings of the inner and outer motor are connected in series, shortening the end-winding length. A flux-switching PM machine with a double C-hoop stator and interior PMs was designed to enhance efficiency and power density,

Received 2023-09-21, **Revised** 2024-01-22.

Biography: Fu Mingzhi (1979—), male, master, senior engineer, mz_fu@qny.chng.com.cn.

Foundation item: National Key Research and Development Plan of China (No. 2020YFB1506603).

Citation: Fu Mingzhi, Qin Meng, Guo Xiaojiang, et al. Magnetic field and coupling effect analysis of a novel dual-rotor dual-stator permanent magnet synchronous generator [J]. Journal of Southeast University (English Edition), 2024, 40(1): 89 - 96. DOI: 10.3969/j.issn.1003 - 7985.2024.01.010.

which is targeted at wind power applications[11]. Asefi et al.[12] studied the topology design and optimization of a dual-rotor axial-flux PM generator. A double-rotor transverse flux PM wind power generator was proposed, and the optimization of rotor width was accomplished to reduce the harmonic component of electro-motive force (EMF)[13].

Based on the structural design, scholars have undertaken extensive theoretical research on DSPMMs and DRPMMs, including analytical models, electromagnetic performance analysis, control system simulation, optimization design, and so forth. Hassannia[14] designed a fractional slot DRPMM to overcome the drawback of high-order harmonics existing in normal DRPMMs with two rotors rotating in opposite directions, whose torque ripple is reduced with double-layer windings. To study the slot-pole combination of DRPMMs for wind power generation, the influence of pole and slot numbers on the winding factor was elaborated, and cogging torque, EMF, and losses were obtained through the finite element method[15]. Wang et al.[16] studied the relationship between the cogging torque and design parameters of a magnetic-geared DRPMM, including the number of slots and poles, airgap magnetic density, and stator tooth width. An optimization simulation of radial-flux DRPMM was performed to minimize the cogging torque and the optimal shift angle of stators[17]. The analytical design of an axial-flux DRPMM was proposed with the dimensioning equations of the machine extracted, and its optimization was performed by using a genetic algorithm[18]. Yang et al.[19] proposed a DRPM vernier machine, and the optimization process of the stator slot was introduced based on a genetic algorithm.

Previous research studies on PM machines with relatively complex structures are mainly focused on dual-stator single-rotor or dual-rotor single-stator types. The former type can either choose two sets of windings for each stator to arrange split control systems or adopt only one set of windings to reduce the length of winding ends, while the latter can accomplish the counterrotation of rotors to meet the special needs of certain application scenarios[20-21]. However, both types lack the advantages of dual-rotor dual-stator (DRDS) PM machines. Some scholars have conducted the topology design of DRDS-PMM for hybrid electric vehicles, wherein a magnetic insulating layer is set to prevent electromagnetic interference and support the inner stator core[22]. Others have devoted themselves to the design process of DRDS flux-switching PM machines for counter-rotating wind turbines[23]. Two six-phase DRDS-PMSGs with different pole configurations were investigated and assessed based on a series of electromagnetic characteristics, including torque, flux density, and efficiency[24]. Currently, the design and analysis of large-scale DRDS-PMSGs are insufficient, and the coupling relation between the inner and outer machines must also be investigated.

The purpose of this study is to investigate a novel DRDS-PMSG for large-scale offshore wind turbines. The analytical model of the generator is established by using an equivalent magnetic circuit method. The electromagnetic characteristics of the generator are evaluated in detail, and the coupling effect between the inner and outer machines is also investigated through finite element analysis.

1 Topology and Main Parameters of the Proposed DRDS-PMSG

1.1 Performance requirements

The proposed DRDS-PMSG is designed for offshore wind power generation and mainly consists of four parts, namely, inner and outer rotors and inner and outer stators. The inner rotor and stator constitute the inner machine, while the outer rotor and stater constitute the outer machine. The main performance requirements of the generator are tabulated in Table 1.

Table 1 Performance requirements of the proposed DRDS-PMSG

Parameters	Inner machine	Outer machine
Number of phases	3	3
Number of poles	12	12
Rated power/kW	750	1 500
Rated speed/(r · min^{-1})	700	600
Rated voltage/V	690	690
Phase current/A	657.7	1 343.7
Peak current/A	930	1 900
Base frequency/Hz	70	60
Power factor	0.99	0.97
Winding connection	Y	Y

The generator has two sets of wind blade systems, which enable the counterrotation of the inner rotor and the outer rotor, thus improving the power generation capacity of the turbine. The structure of dual airgaps effectively increases the airgap area, thereby raising the torque and power densities so that it can output more power from the dual electrical ports at the same volume and material consumption condition. The adoption of a surface-mounted PM structure can reduce the cogging torque of the machine compared with an interior PM structure. In addition, since the length of the winding end does not change with the machine length, the torque density can be further improved by increasing the length-diameter ratio.

1.2 Topology, structural parameters, and winding schemes

The cross-section of the proposed DRDS-PMSG is shown in Fig. 1. The inner and outer machines are inner- and outer-rotor machines. A layer of flux shield exists between the inner and outer machines to eliminate the coupling effect between the magnetic fields of the inside and outside machines. In addition, the inner and outer ma-

chines are equipped with a set of windings. The conductors in the inner and outer stator slots constitute the inner and the outer machine stator windings, respectively. The two sets of windings are electrically independent of each other to generate output currents with different frequencies through the rotation of the front and rear wind blades at different speeds.

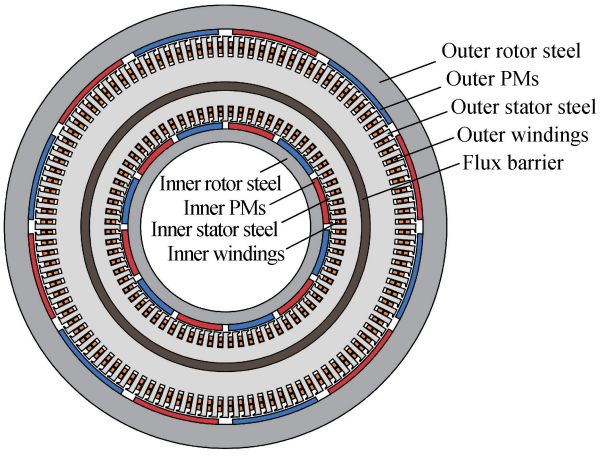

Fig. 1 Cross-section of the proposed DRDS-PMSG

The main structural parameters and designed winding schemes are tabulated in Tables 2 and 3.

Table 2 Structural parameters of the proposed DRDS-PMSG

Parameters	Inner machine	Outer machine
Rotor inner diameter/mm	500	1 160
Rotor outer diameter/mm	574	1 300
Stator inner diameter/mm	620	850
Stator outer diameter/mm	800	1 118
Stack length/mm	750	750
Magnet thickness/mm	18	15
Airgap length/mm	5	6

Table 3 Winding schemes of the proposed DRDS-PMSG

Parameters	Inner machine	Outer machine
Number of stator slots	72	108
Number of conductors per slot	8	6
Number of coils per phase per pole	2	3
Number of parallel branches	6	6
Coil pitch	6	9

2 Modeling of the Proposed DRDS-PMSG

The preliminary theoretical analysis of DRDS-PSMGs is typically based on an equivalent magnetic circuit model. According to the magnetic circuit structure of the generator, its magnetic field is divided into three parts: inner airgap field region, outer airgap field region, and coupling field region, based on which the equivalent magnetic circuit model is established.

2.1 Reluctance formulas of the magnetic field

The distribution of the inner airgap magnetic field is similar to that of the outer airgap magnetic field; the equivalent magnetic circuits of the inner and outer machines are thus analogical. Taking the outer machine as an example, the magnetic circuit division includes the PM, rotor core, airgap, stator core, and magnetic field coupling regions.

Based on the equivalent magnetic circuit model in Fig. 2, the reluctance formulas of all parts in the flux paths can be obtained. The reluctance formula of the PM region can be expressed as follows:

$$R_{\mathrm{pm}}=\frac{h_{\mathrm{pm}}}{\mu_{\mathrm{pm}}\alpha\tau L} \tag{1}$$

where h_{pm} is the thickness of PMs, μ_{pm} is the permeability of PMs, α is the pole-arc coefficient, τ is the pole pitch, and L represents the axial length of the machine core.

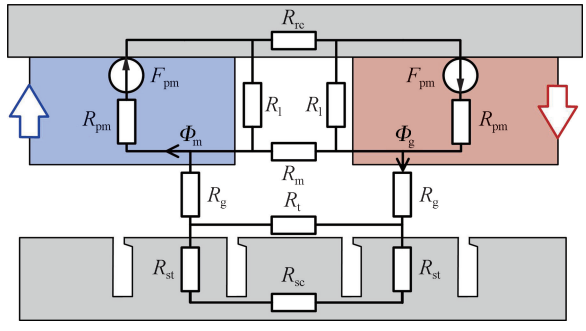

Fig. 2 Equivalent magnetic circuit diagram of the DRDS-PMSG (outer machine)

The reluctance formula of the rotor yoke region can be expressed as follows:

$$R_{\mathrm{rc}}=\frac{l_{\mathrm{rc}}}{\mu_{\mathrm{rc}}h_{\mathrm{rc}}L_{\mathrm{ef}}} \tag{2}$$

where l_{rc} is the circumferential length of the inner and outer rotors for each pair of poles, μ_{rc} is the permeability of the rotor yoke, h_{rc} is the thickness of the rotor core, and L_{ef} represents the effective axial length of the machine.

The reluctance formulas of the airgap region can be expressed as follows:

$$R_{\mathrm{g}}=\frac{g}{\mu_0\tau L} \tag{3}$$

where g is the length of airgap, μ_0 is the permeability of vacuum.

The reluctance formulas of the stator yoke region can be expressed as follows:

$$R_{\mathrm{sc}}=\frac{l_{\mathrm{sc}}}{\mu_{\mathrm{sc}}h_{\mathrm{sc}}L_{\mathrm{ef}}} \tag{4}$$

where l_{sc} is the circumferential length of the stator for each pair of poles, μ_{sc} is the permeability of the stator yoke, and h_{sc} is the thickness of the stator core.

The airgap flux density of the machine can be calculated by the following:

$$B_{\mathrm{g}}=\frac{\Phi_{\mathrm{g}}}{\alpha\tau L} \tag{5}$$

where Φ_g is the airgap flux.

2.2 Overall equivalent magnetic circuit model

Since the inner and outer rotors rotate in opposite directions, the relative positions of the inner and outer PMs will change with their rotation. Flux leakages exist in the flux barrier between inner and outer stators, so it is necessary to further establish the coupled magnetic field model. The typical relative positions of inner and outer PMs are shown in Fig. 3, which include three situations: PMs aligned with the same polarity, PMs aligned with a different polarity, and PMs unaligned. In Fig. 3(a), the inner and outer PMs are aligned with the same polarity, which indicates that the overall magnetic circuit of the machine is in parallel connection, the coupling degree in the radial direction is relatively low; therefore, the reluctance in the coupling area is regarded as circumferential reluctance. In Fig. 3(b), the overall magnetic circuit is in a series connection, while in Fig. 3(c), the inner and outer PMs are not mutually aligned. In Figs. 3(b) and 3(c), the magnetic field coupling exists in the radial direction; therefore, the reluctance in the coupling region is set as radial reluctance.

In the operation process of the generator, the different

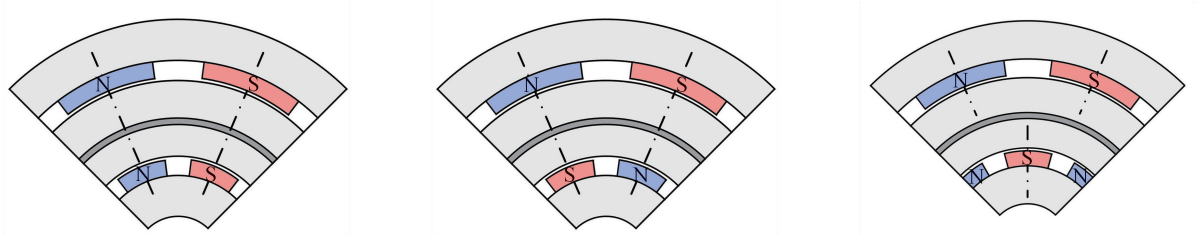

(a) (b) (c)

Fig. 3 Typical relative positions of inner and outer PMs of the DRDS-PMSG. (a) PMs aligned with the same polarity; (b) PMs aligned with the different polarity; (c) PMs not aligned

relative positions of the inner and outer PMs lead to different saturation conditions of the stator yoke cores. The circumferential stator yoke flux in parallel magnetic circuits is larger than that in series and general magnetic circuits. Therefore, the magnetic field of the yoke core is most possibly saturated in Fig. 3(a). According to the PMs' relative positions of the inner and outer machines, the equivalent reluctance of the coupling region can be obtained by

$$R_s = \begin{cases} \dfrac{l_s}{\mu_s \pi h_s L_{ef}} & \Delta\theta = 0 \\ \dfrac{4ph_s}{k_s \mu_s \pi (D_{os1} + D_{is2}) L_{ef}} & \Delta\theta \in [-90°, 0) \cup (0, 90°] \end{cases} \tag{6}$$

where l_s is the circumferential length between the two adjacent poles of the magnetic coupling region, μ_s is the permeability of the flux barrier, h_s is the width of the flux barrier, p is the number of pole pairs, k_s is equivalent reluctance correction coefficient, D_{os1} is the inner diameter of the outer stator, D_{is2} is the outer diameter of the inner stator, and $\Delta\theta$ is the relative electrical angle of the inner and outer rotor. The range of $\Delta\theta$ is converted from $[-180°, 180°]$ to $[-90°, 90°]$, according to the symmetric polarity of the PMs. The initial reference state of $\Delta\theta$ is where PMs are aligned with the same polarity.

As mentioned before, since the relative positions of inner and outer PMs change constantly, the correction coefficient of equivalent reluctance in the coupling region also changes, which can be obtained by

$$k_s = \begin{cases} (0.037h_s + 0.5)\sin(7.92 \times 10^{-4} n_r \Delta\theta + 0.027\pi) & \Delta\theta \in [-90°, 0) \\ (0.037h_s + 0.5)\sin(7.92 \times 10^{-4} n_r \Delta\theta - 0.027\pi) & \Delta\theta \in (0, 90°] \end{cases} \tag{7}$$

where n_r is the relative speed between the inner and outer machines.

Thus, the overall equivalent magnetic circuit model of the DRDS-PMSG can be obtained, as shown in Fig. 4.

3 Coupling Effect Analysis of the Proposed DRDS-PMSG

To explore the coupling effect of the proposed DRDS-PMSG, its electromagnetic characteristics are evaluated through finite element analysis (FEA), including flux density distribution, airgap flux density, EMF, and cogging torque.

3.1 Magnetic field distributions

Figs. 5 and 6 show the magnetic flux and flux density distributions of the generator in no-load and full-load conditions. The maximum flux density of the generator in the no-load condition is at the outer stator tooth (1.92 T), while the maximum flux density at the full-load condition is also at the outer stator tooth (1.98 T). The average values of airgap flux density under the three different PM relative positions in no-load condition remain almost the same, while in full-load condition, the corresponding values when the PMs are aligned with the same polarity

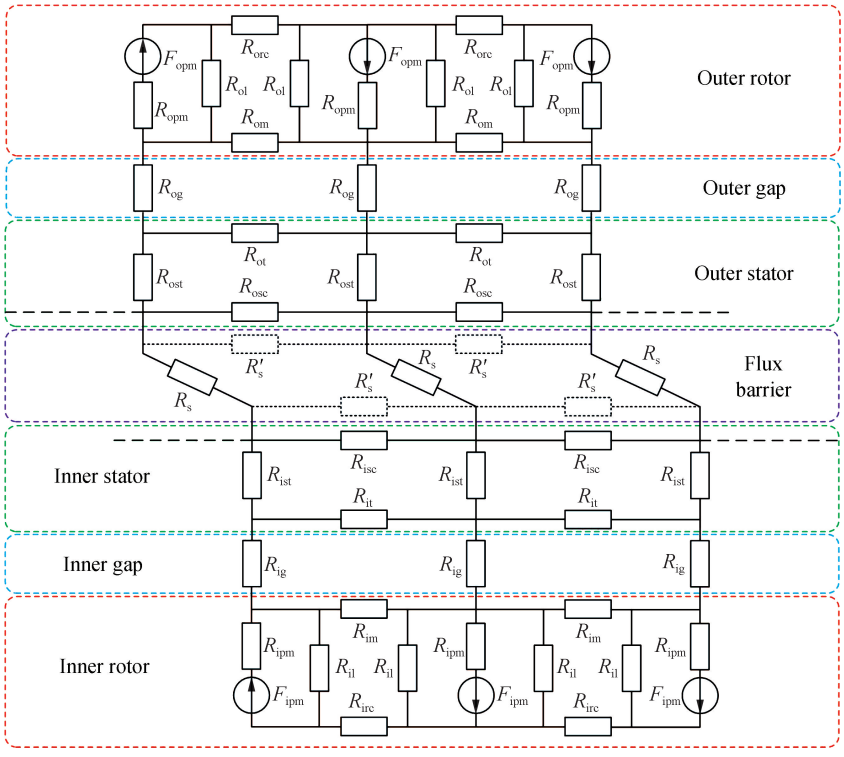

Fig. 4 Overall equivalent magnetic circuit model of the DRDS-PMSG

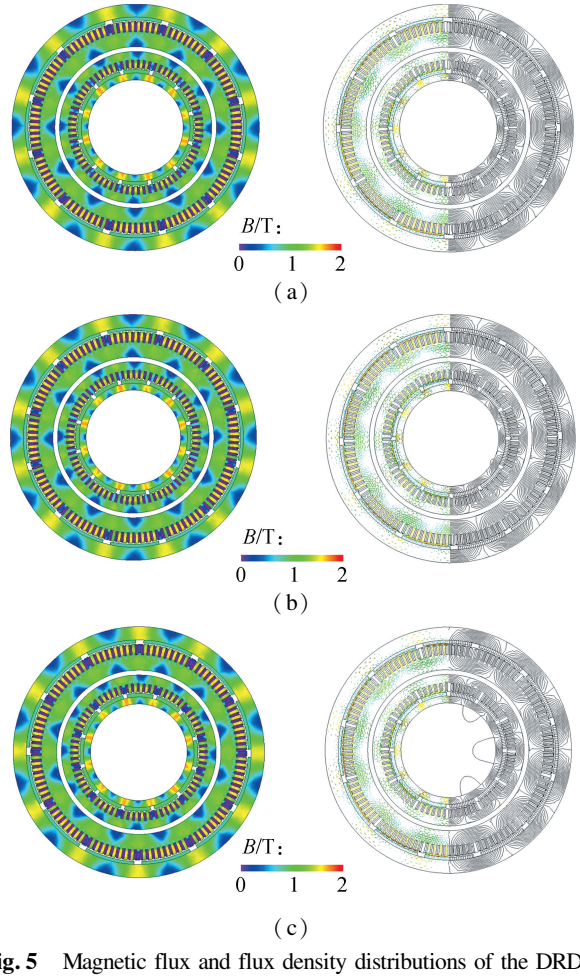

Fig. 5 Magnetic flux and flux density distributions of the DRDS-PMSG in no-load condition. (a) PMs aligned with the same polarity; (b) PMs aligned with the different polarity; (c) PMs not aligned

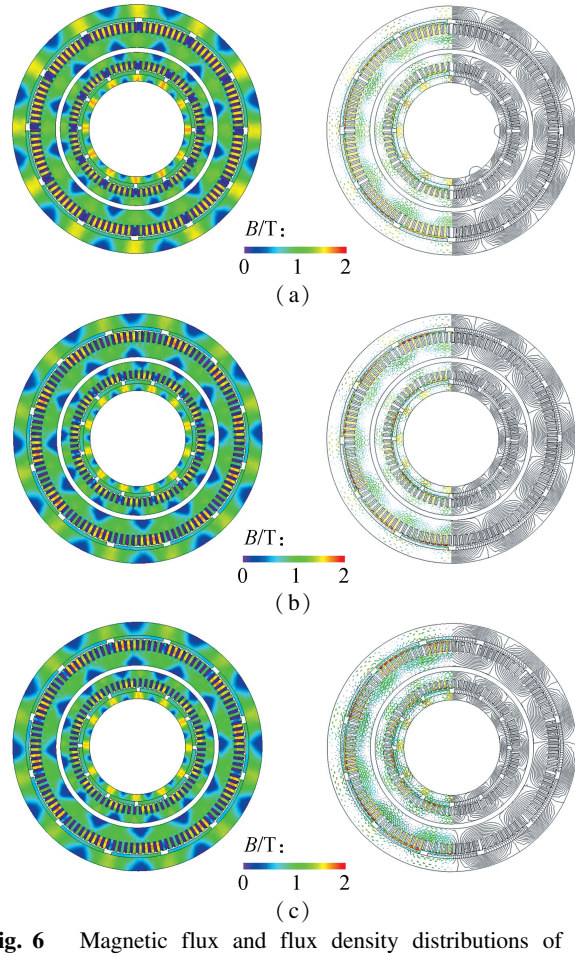

Fig. 6 Magnetic flux and flux density distributions of the DRDS-PMSG at full-load condition. (a) PMs aligned with the same polarity; (b) PMs aligned with the different polarity; (c) PMs not aligned

are slightly smaller than those when the PMs are aligned with different polarity or not aligned. Therefore, flux leakages exist in the flux barrier, which will cause a difference in the airgap flux density.

3.2 Electromagnetic characteristics

Figs. 7 and 8 show the waveforms and harmonic contents of inner and outer airgap flux densities in no-load conditions under different PM relative positions. Evidently, the fundamental amplitude of the inner air-gap magnetic flux density when the PMs are aligned with the same polarity is slightly higher than that when the PMs are aligned with different polarity or not aligned, while the fundamental amplitudes of the outer air-gap magnetic flux density of the three typical PMs relative positions remain almost the same.

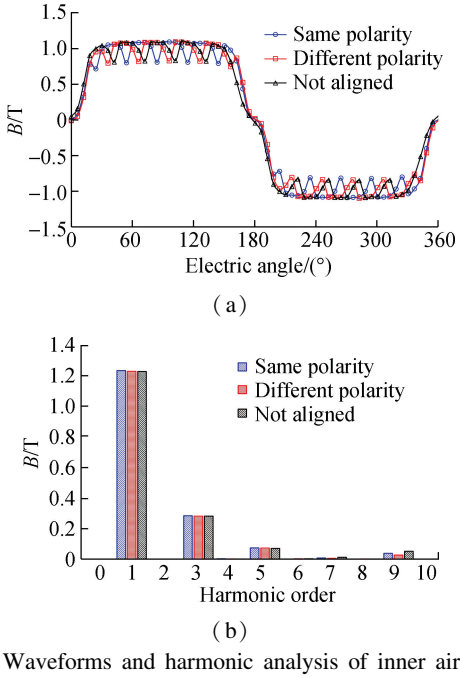

Fig. 7 Waveforms and harmonic analysis of inner airgap flux density. (a) Waveforms; (b) Harmonics

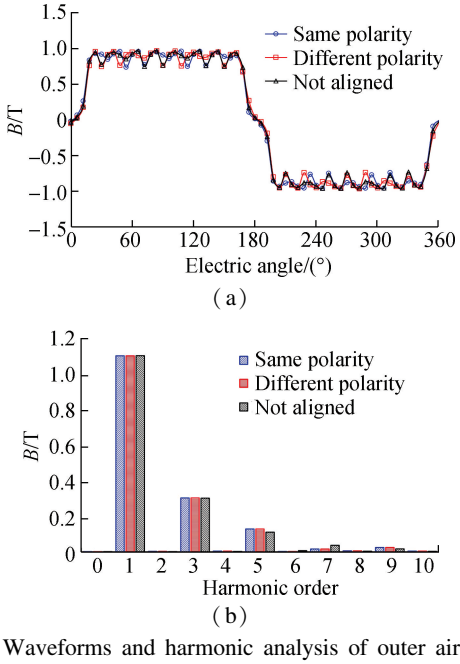

Fig. 8 Waveforms and harmonic analysis of outer airgap flux density. (a) Waveforms; (b) Harmonics

Fig. 9 shows the waveforms and harmonic contents of the inner and outer EMFs. It shows that the waveforms are almost the same under single-machine simulation and double-machine simulation, indicating that the magnetic circuit coupling has little effect on the fundamental magnitudes of EMFs.

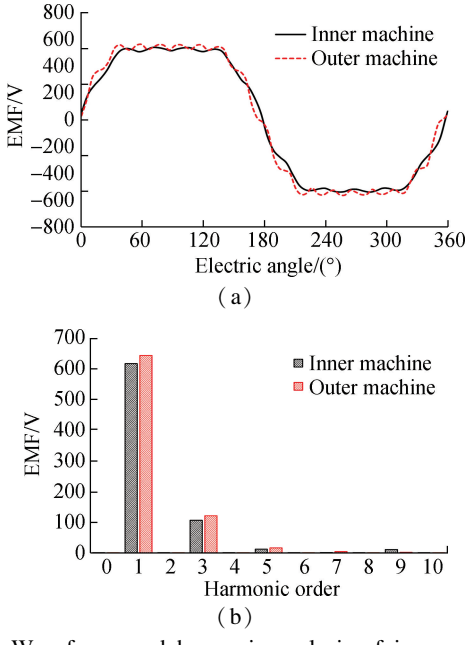

Fig. 9 Waveforms and harmonic analysis of inner and outer EMFs. (a) Waveforms; (b) Harmonics

Fig. 10 shows the cogging torque waveforms of the generator. Evidently, the peak-to-peak value of the cogging torque of the inner machine is 0.52 kN · m, lower than the 1.64 kN · m of the outer machine. Fig. 11 shows the torque waveforms of the generator. The average value of the inner machine is 11.65 kN · m, compared with 27.09 kN · m of the outer machine. The torque ripples of the inner and outer machines are calculated as 6.02% and 4.12%, respectively. Fig. 12 shows the FEA-predicted and experimentally measured no-load characteristics of the machine, both of which are in good agreement.

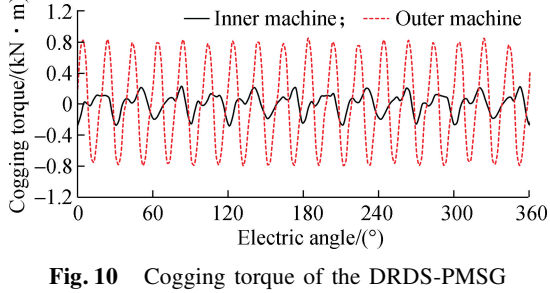

Fig. 10 Cogging torque of the DRDS-PMSG

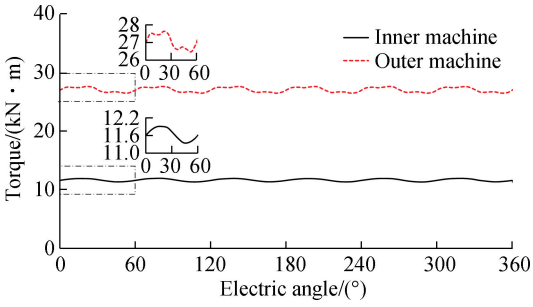

Fig. 11 Torque of the DRDS-PMSG

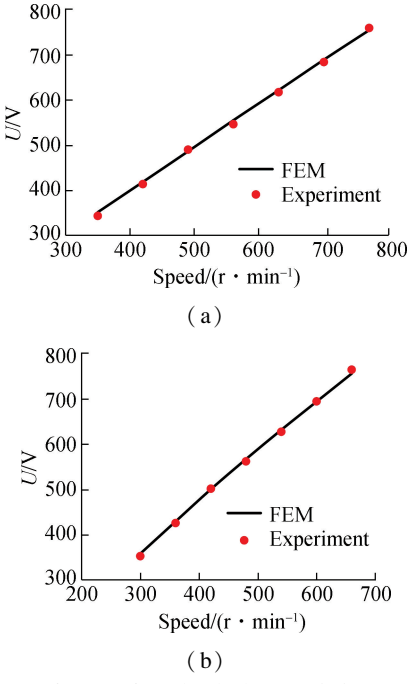

Fig. 12 Waveforms of no-load characteristic. (a) Inner machine; (b) Outer machine

4 Conclusions

1) The leakage flux exists in the flux shield between the inner and outer machines, but due to the isolation effect of the flux barrier, the coupling effect is greatly reduced. However, the magnetic field of the inner machine is still influenced by the leakage flux of the outer magnetic circuit to some extent.

2) The flux density and EMF waveforms are similar under the three typical relative positions, mainly containing odd harmonic components.

3) The peak-to-peak value of cogging torque of the inner machine is lower than that of the outer machine, with the inner and outer machines reaching 0.52 and 1.64 kN · m, respectively. The torque ripple of the inner machine is 6.02%, which is slightly higher than the torque ripple of 4.12% of the outer machine.

References

[1] Wang X P, Zhao J, Wang B H, et al. Predictive current control system of PMSM based on LADRC[J]. *Journal of Southeast University* (*English Edition*), 2022, **38**(3): 227 − 234. DOI: 10.3969/j.issn.1003-7985.2022.03.003.

[2] Lin H Y, Guo Y J, Sun B B, et al. Overview of offshore wind power key technologies[J]. *Journal of Southeast University* (*Natural Science Edition*), 2011, **41**(4): 882 − 888. DOI: 10.3969/j.issn.1001-0505.2011.04.042. (in Chinese)

[3] Zhang P Y, Ding H Y, Le C H, et al. Towing characteristics of large-scale composite bucket foundation for offshore wind turbines[J]. *Journal of Southeast University* (*English Edition*), 2013, **29**(3): 300 − 304. DOI: 10.3969/j.issn.1003-7985.2013.03.013.

[4] Kumar R R, Devi P, Chetri C, et al. Design and characteristics investigation of novel dual stator pseudo-pole five-phase permanent magnet synchronous generator for wind power application[J]. *IEEE Access*, 2020, **8**: 175788 − 175804. DOI: 10.1109/ACCESS.2020.3025842.

[5] Kim G H, Jung T U. Stator teeth pairing design for reduction of cogging torque of dual RFPM generator[C]// 2020 *IEEE 19th Biennial Conference on Electromagnetic Field Computation* (*CEFC*). Pisa, Italy, 2020: 1 − 4. DOI: 10.1109/CEFC46938.2020.9451318.

[6] Pramurti A R, Firmansyah E, Suharyanto. Reduction on cogging torque in dual stator radial flux permanent magnet generator for low speed wind turbine[C]//2016 *3rd International Conference on Information Technology, Computer, and Electrical Engineering* (*ICITACEE*). Semarang, Indonesia, 2017: 1 − 4. DOI: 10.1109/ICITACEE.2016.7892434.

[7] Wei S H, Xu Y L, Tian X. Presentation of a double-stator axial-flux permanent-magnet disk motor with soft magnetic composite cores and its cogging torque reduction [C]//2019 *22nd International Conference on Electrical Machines and Systems* (*ICEMS*). Harbin, China, 2019: 1 − 4. DOI: 10.1109/ICEMS.2019.8921831.

[8] Yu J C, Liu C H. Multi-objective optimization of a double-stator hybrid-excited flux-switching permanent-magnet machine[J]. *IEEE Transactions on Energy Conversion*, 2020, **35**(1): 312 − 323. DOI: 10.1109/TEC.2019.2932953.

[9] Zhang K H, Fang Y T, Huang X Y, et al. Design of a dual-stator superconducting permanent magnet wind power generator with different rotor configuration[C]//2016 *IEEE Conference on Electromagnetic Field Computation* (*CEFC*). Miami, FL, USA, 2016: 1. DOI: 10.1109/CEFC.2016.7816300.

[10] Allahyari A, Torkaman H. A novel high-performance consequent pole dual rotor permanent magnet vernier machine[J]. *IEEE Transactions on Energy Conversion*, 2020, **35**(3): 1238 − 1246. DOI: 10.1109/TEC.2020.2980146.

[11] Jia Z, Lin H Y, Fang S H, et al. Cogging torque optimization of novel transverse flux permanent magnet generator with double C-hoop stator[J]. *IEEE Transactions on Magnetics*, 2015, **51**(11): 8208104. DOI: 10.1109/TMAG.2015.2453052.

[12] Asefi T, Faiz J, Khan M A. Design of dual rotor axial flux permanent magnet generators with ferrite and rare-

earth magnets[C]//2018 *IEEE* 18*th International Power Electronics and Motion Control Conference* (*PEMC*). Budapest, Hungary, 2018: 531 - 538. DOI: 10.1109/EPEPEMC.2018.8522004.

[13] Ali Noroozi M, Milimonfared J, Yazdanpanah R. Novel double-sided disk-shaped passive-rotor transverse-flux permanent magnet generators for wind turbine applications [C]//2020 11*th Power Electronics, Drive Systems, and Technologies Conference* (*PEDSTC*). Tehran, Iran, 2020: 1 - 4. DOI: 10.1109/PEDSTC49159.2020.9088467.

[14] Hassannia A. Conceptual design of fractional slot concentrated winding dual-rotor double-speed synchronous motor [J]. *IEEE Transactions on Energy Conversion*, 2020, **35**(2): 986 - 993. DOI: 10.1109/TEC.2019.2956073.

[15] Xu P F, Shi K, Sun Y X, et al. Effect of pole number and slot number on performance of dual rotor permanent magnet wind power generator using ferrite magnets[J]. *AIP Advances*, 2017, **7**(5): 056631. DOI: 10.1063/1.4974497.

[16] Wang Q S, Niu S X, Yang L. Design optimization of a novel scale-down hybrid-excited dual permanent magnet generator for direct-drive wind power application[J]. *IEEE Transactions on Magnetics*, 2018, **54**(3): 8100904. DOI: 10.1109/TMAG.2017.2758021.

[17] Kumar P, Reza M M, Srivastava R K. Analytical method for calculation of cogging torque reduction due to slot shifting in a dual stator dual rotor permanent magnet machine with semi-closed slots[J]. *Progress In Electromagnetics Research M*, 2018, **70**: 99 - 108. DOI: 10.2528/pierm18050506.

[18] Akinci R, Polat M. Design and optimization with genetic algorithm of double rotor axial flux permanent magnet synchronous motor (TORUS type) for electrical vehicles [C]//2019 4*th International Conference on Power Electronics and their Applications* (*ICPEA*). Elazig, Turkey, 2019: 1 - 5. DOI: 10.1109/ICPEA1.2019.8911175.

[19] Yang K, Zhao F, Wang Q L, et al. Optimization design of a dual-rotor axial-flux permanent magnet vernier machine based on genetic algorithm[C]//2019 22*nd International Conference on Electrical Machines and Systems* (*ICEMS*). Harbin, China, 2019: 1-5. DOI: 10.1109/ICEMS.2019.8922135.

[20] Ullah W, Khan F, Hussain S. Dual mechanical port power distribution in dual rotor permanent magnet flux switching generator for counter-rotating wind turbine applications[J]. *IET Renewable Power Generation*, 2022, **16**(6): 1087 - 1278. DOI: 10.1049/rpg2.12447.

[21] Luo X, Niu S X. A novel contra-rotating power split transmission system for wind power generation and its dual MPPT control strategy[J]. *IEEE Transactions on Power Electronics*, 2017, **32**(9): 6924 - 6935. DOI: 10.1109/TPEL.2016.2629021.

[22] Muteba M. Dual stator dual rotor interior permanent magnet synchronous motor for hybrid electric vehicles[C]//2020 *IEEE Transportation Electrification Conference & Expo* (*ITEC*). Chicago, IL, USA, 2020: 462 - 465. DOI: 10.1109/ITEC48692.2020.9161707.

[23] Ullah W, Khan F, Hussain S. A comparative study of dual stator with novel dual rotor permanent magnet flux switching generator for counter rotating wind turbine applications[J]. *IEEE Access*, 2022, **10**: 8243 - 8261. DOI: 10.1109/ACCESS.2022.3143166.

[24] Kumar R R, Kumari A, Dutta S, et al. Design and comparative analysis of halbach array and surface mounted magnetic pole dual rotor de-coupled stator six-phase permanent magnet synchronous generator for wind power application[C]//2020 *IEEE International Conference on Power Electronics, Drives and Energy Systems* (*PEDES*). Jaipur, India, 2020: 1 - 6. DOI: 10.1109/PEDES49360.2020.9379803.

新型双转子双定子永磁同步发电机的磁场及耦合效应分析

付明志[1] 秦 猛[1] 郭小江[1] 陈雨菡[2] 林鹤云[2]

([1] 华能清洁能源技术研究院,北京 100032)

([2] 东南大学电气工程学院,南京 210096)

摘要:为了解决目前海上风力发电机存在的成本高、体积大等问题,提出一种新型双转子双定子永磁同步发电机(DRDS-PMSG).建立了发电机的等效磁路模型,采用有限元分析方法评估了发电机的电磁特性及内外电机的耦合效应,部分仿真结果得到了实验验证.仿真结果表明:随着内、外永磁体相对位置的改变,电机等效磁路存在3种典型情况,并可通过耦合系数对耦合区域的等效磁阻进行描述;内、外电机的耦合效应体现在齿槽转矩、电磁转矩等电磁特性上,内、外电机的齿槽转矩峰峰值分别为0.52和1.64 kN·m,电磁转矩平均值分别为11.65和27.09 kN·m,转矩脉动分别为6.02%和4.12%;总体来看,内、外电机之间存在一定程度的耦合,但该耦合效应被隔磁环有效削弱.

关键词:双转子双定子;电磁特性;永磁同步发电机;磁场;有限元分析;耦合效应

中图分类号:TM315